The probability of long phases without wind power and their impact on an energy system with high share of renewable energies

Patrick Plötz*, Julia Michaelis

Fraunhofer Institute for Systems and Innovation Research ISI,
Breslauer Strasse 48, 76139 Karlsruhe, Germany

Abstract

Long phases of no or little wind power are a potential thread to future energy systems with a high share of renewable energies. A frequently cited example observed in Germany was a whole week with very little wind power due to temperature inversion in January 2009. A frequent occurrence of these and similar situations would imply an increased need for energy storage or controllable power capacities in order to cover energy demand at any time in future energy systems.

Energy system research analyses the future effect of high renewable feed-in using mainly historical weather or renewable energy feed-in time series data. However, an understanding of the representativeness with respect to extreme weather events and long phases of low wind speeds or calms is still limited. Here, we study the frequency of occurrence of long calms in wind power feed-in and residual load as well as differences in their frequency of occurrence between different years. We analyse seven years of aggregated wind power feed-in in Germany on an hourly basis. We discuss the occurrence of extreme events in low wind and renewable power feed-in as observed historically for different threshold levels of low feed-in. In addition to this, we use extreme value statistics to obtain reliable estimates for extreme events such as hundred year calms.

We find the average duration of low wind power feed-in phase to grow linearly with the threshold: Phases with a wind power feed-in of less than two percent of installed power are typically four hours long and phases with less than five percent feed-in are on average seven hours long. However, a period of wind power feed-in below eight percent of installed power that lasts one week occurs every two years and a period of more than ten days occurs every ten years.

Keywords: wind power, calm, extreme value statistics, energy system analysis

*Corresponding author
Email address: patrick.ploetz@isi.fraunhofer.de (Patrick Plötz)

1. Introduction

Future energy systems will largely depend on renewable electricity generation. For the case of Germany, long phases of little or now wind are a potential thread to the security of electricity supply. For example, an atmospheric inversion led to one week with almost no wind in Germany in January 2009 despite the fact that wind power feed-in is usually high in winter times. Additionally, higher volatility of power sources implies a higher flexibility of the energy systems.

Present day energy system research uses historical weather or renewable feed-in time series data to analyse possible future energy systems [1, 2]. However, little is known about the actual representativeness of these time series beyond average wind speeds and associated power feed-in. In particular the frequency and duration of extreme events such as long periods of low wind speeds and low renewable feed-in have not been analysed in detail yet. And yet the latter are important to understand and evaluate the outcomes of complex energy system models. At present, complex energy system models optimise whole energy systems but the impact and details of how to arrive from a particular weather time series at a full energy system is involved and almost impossible to trace.

Wind speeds and extreme weather events have been studied by statistical methods including extreme value theory (EVT) [3, 4, 5]. However, the focus of these studies is either on the statistical distribution of wind speeds [6] or the probability of very high wind speeds. The occurrence and duration of phases with low or now wind and their consequences for energy system models has – to our knowledge – not been analysed yet. Similarly, EVT applications to climate or weather mainly focus on extremely high wind speeds or floods or both. It has been argued that climate change alters the wind speeds and patterns but current research on this topic is not conclusive yet [7].

Here, we analyse the frequency and duration of long phases of low wind power feed-in and residual load for Germany. The data for our analysis covers seven years of renewable generation from Germany and is presented in section 2 together with an outline of the statistical methods used in our analysis. The following section 3 contains the results on the frequency and duration of phases with little wind power feed-in and low residual load. We close with a discussion and summary in section 4.

2. Data and Methods

2.1. Wind power feed-in and residual load time series data

We use wind power feed in data for seven years from Germany from 2006–2012. These time series include the feed-in of wind power stations that are located onshore. As the installed capacity of offshore wind power plants account for less than 2% of the installed wind capacity in Germany in 2014, the feed-in of these offshore wind parks is not considered [8]. Extrapolations of wind power feed-in are published on-line by the four national transmission system operators with a time resolution of fifteen minutes [9]. These original data is converted into time series with an hourly resolution.

We normalised the wind power feed-in from different years by dividing the annual feed-in by the installed capacity. This makes different years comparable. Since installed wind power grew over time, the annual average wind power feed-in would have increased trivially without normalisation. We obtained the installed capacity for each from [13]

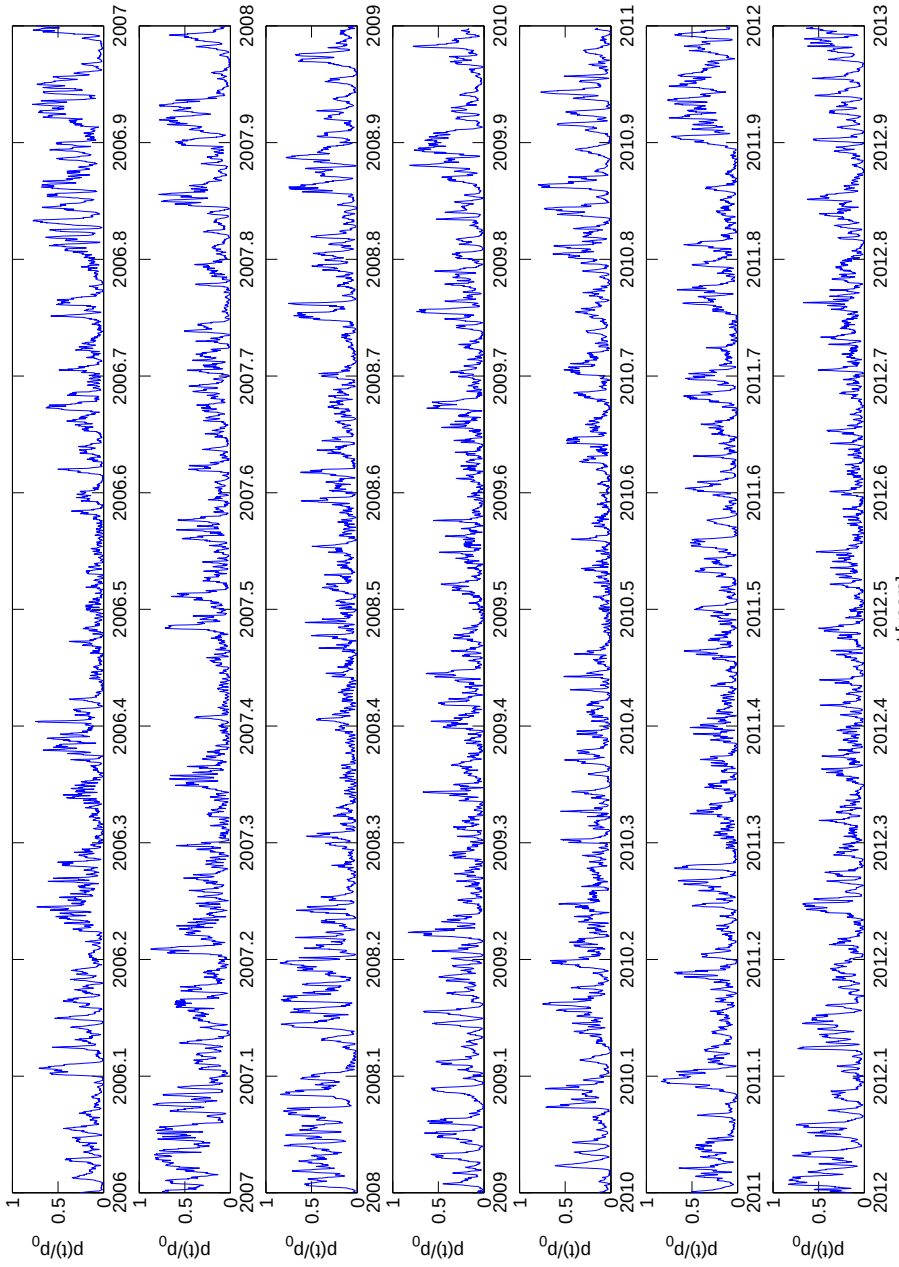

Figure 1: Total normalised wind power feed-in in Germany 2006–2012. A value of 1 would correspond to all wind turbines operating at full power at the same time.

and linearly interpolated over the year. Figure 1 shows the normalised wind power feed-in for all Germany during 2006–2012. At no time during the observation period did all wind turbine operate at full load (as expected) and accordingly the normalised wind

power feed-in never reached 100%. One also observes the well-known seasonal patterns for Germany with higher wind power feed-in during winter.

Figure 2 shows the empirical distribution function of normalised total wind power feed-in in Germany 2006–2012. Typical values range from 5–20% of total installed capacity but the distribution is clearly right skewed higher values of wind power feed-in occur quite frequently, too. The median wind power feed-in is 13.1 % as compared to the mean of 18.2 %. The inset in Figure 2 shows the empirical cumulative distribution func-

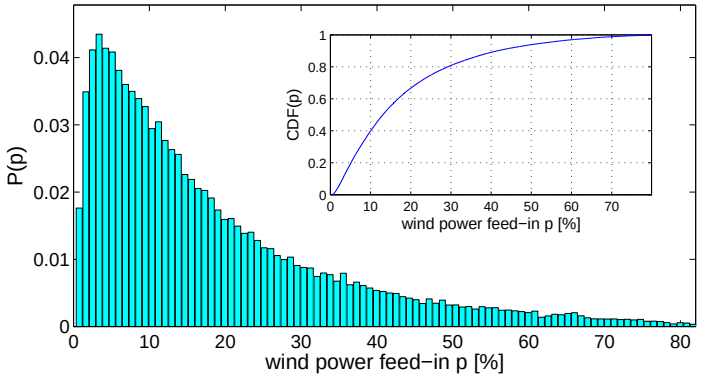

Figure 2: Probability density function for wind power feed-in normalised by the total installed capacity. *Inset*: Cumulative distribution function (CDF) of the normalised wind power feed-in.

p	[%]	1	5	10	15	20	25	50	66
CDF(p)	[%]	2.96	19.2	39.7	55.3	66.5	74.7	93.9	98.2

Table 1: Values of the CDF of normalised total wind power feed-in in Germany 2006–2012.

tion (CDF) of the normalised wind power feed-in in Germany. We observe that 0–10% wind power feed-in occur in 40% of all hours. Very high total wind power feed-in is quite rare, only two percent of all hours exhibit wind power feed-in above 60% of installed capacity.

Residual load time series data have been obtained by combining the wind power feed-in data with solar power and load data. We understand residual load as the net power consumption minus the onshore wind and photo voltaic (PV) power feed-in. The time series for PV feed-in are published on the website mentioned above. As the data is available from March 2011 onwards, we only used the time series of 2012 and scaled it for the preceding years by using the installed PV capacities of the years 2006-2011. Load data for Germany is available on the website of Entso-E [10] for the whole period of 2006–2012. We slightly rescaled the load data to match the German annual electricity consumption [14]. For the phases of low residual load we use the following thresholds: 35, 40, 49, and 60 GW which correspond approximately to the 3, 8, 32, and 64% quantiles.

2.2. Methods

We briefly introduce key concepts from statistics and extreme value theory for later use and to introduce notation.

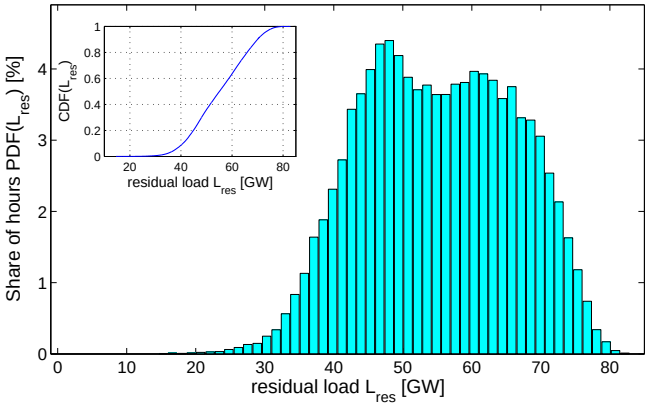

Figure 3: Probability density function of residual load in Germany 2006–2012. *Inset*: Cumulative distribution function (CDF) of residual load.

Quantile	min	0.10	0.25	0.50	0.75	0.90	max
L_{res} [GW]	14.6	40.8	46.5	55.1	64.0	70.0	82.9

Table 2: Quantiles of hourly residual load data in Germany 2006–2012.

Statistical fundamentals

We analyse the probability of long phases with little or no wind power feed-in, so-called calms in case of wind, as well as phases of low residual load. In this context, the probability $\Pr\{T \geq t\}$ of an event with duration of at least t hours is more interesting than the probability of an event of *exactly* t hours. The concepts of survival analysis can be used here and we follow [16] in our presentation.

Let T denote a positive integer random variable, for example the duration of a phase with little wind power feed-in. Quite generally, T could be a real-valued random variable but we will use integer values since all data we use is given in equidistant steps of full hours. Let $f(t) = \Pr\{T = t\}$ denote the probability density function (PDF) for a lifetime T matching exactly t hours. Then $F(t) = \Pr\{T \leq t\} = \sum_{t' \leq t} f(t')$ is the cumulative density function (CDF) or probability distribution function and

$$S(t) = \Pr\{T \geq t\} = \sum_{t' \leq t} f(t') = 1 - F(t) \tag{1}$$

denotes the *survivor function*. The latter is the probability of observing a phase of at least t hours [16]. It is useful to be aware of the uncertainty of this estimator. With the number of failures d_j and sample size n_j in time step j, the variance of $S(t)$ can be estimated as

$$\hat{\sigma}_S^2 = \widehat{\mathrm{Var}}[\hat{S}(t)] = \hat{S}(t)^2 \sum_{j<t} \frac{d_j}{n_j(n_j - d_j)} = \hat{S}(t)(1 - \hat{S}(t))/n \tag{2}$$

and asymptotic confidence intervals $\hat{S}(t) - t_{1-\alpha}(n-1)\hat{\sigma}_S < S(t) < \hat{S}(t) + t_{1-\alpha}(n-1)\hat{\sigma}_S$ can be given using Student's $t_x(n)$ function [16]. The result in Eq. (2) is known as Greenwood formula. The last equality holds if the data are not censored [16, S. 82].

Extreme value statistics

Extreme value theory provides statistical tools to quantify the behaviour of a process at extremely large values [11]. We will briefly review some key concepts for the reader to understand the methods used to obtain the results in section 3.

Two methods are used in extreme value analysis to estimate the asymptotic distribution of extreme for a given problem: the block maxima method and peak-over-threshold method. For the first method, the times series is divided in intervals of common length such as years or months and the maxima within this block of data are further analysed with the help of asymptotically correct distributions for the maxima. This has the advantage of simple interpretation but only a single data point is used from each interval. For the peak-over-threshold method, all data above a fixed threshold are used and their distribution function is similarly analysed with asymptotic distributions. The choice of threshold can be difficult in applications but more of the data is used. Since we are interested in long periods of little wind power feed-in or residual load which can – depending on the definition of 'low' – extend over one week or longer, the peak-over-threshold is more suitable.

Let $X_1, \ldots, X_n$ denote a series of iid random variables with CDF $F(x)$. We consider those values as extreme that lie above a certain threshold u. The distribution of extreme values X, i.e. the probability to lie at least $y > 0$ above the threshold if $X > u$, is given by

$$\Pr\{X > u + y | X > u\} = \frac{1 - F(u + y)}{1 - F(u)}. \tag{3}$$

However, the original distribution function $F(x)$ is usually not known in applications. The interesting results of extreme value theory [11] is that the distribution of $x = X - u$ conditioned to $X > u$, i.e. $\Pr\{x = X - u | X > u\}$, is asymptotically for large u given by

$$H_u(x) = 1 - \left(1 + \frac{\xi x}{\tilde{\sigma}}\right)^{-1/\xi} \tag{4}$$

for $x > 0$, $1 + \xi x/\tilde{\sigma} > 0$ and $\tilde{\sigma} = \sigma + \xi(u - \mu)$. The distribution in eq. (4) is known as *generalised Pareto distribution*. If $\xi = 0$ the distribution is given by $H_u(x) = 1 - \exp(-x/\tilde{\sigma})$, $x > 0$, which is an exponential distribution of the extreme values.

In the application, a threshold u dividing extreme and normal values has to be defined. Different methods have been discussed in the literature. A common method is to use all values greater than some quantile of the data, e.g. to use the largest 20 % of the data as extreme. This method has been used for the results in section 3. We checked the robustness of the results in section 3 against the choice of threshold. The parameters of the generalised Pareto distribution have been found by maximum likelihood estimate [11, Kap. 4.3].

Plots of the probability of extreme events are difficult to read since the events of interest have extremely low probability. EVT has developed methods to visualise the likelihood of extreme events in a more accessible way. It is common to display the magnitude of the extreme event as a function of (the logarithm of) the return period as in figure 6. Such a return level plot is easy to read and the predicted magnitude of extreme events using the GPD can easily be integrated. For $\xi = 0$ the GPD corresponds to linear dependence in a return level plot. More precisely, the probability of observing an extreme greater x, conditioned to $x > u$, equal to $\Pr\{X > x | x > u\} = [1 - \xi(\frac{x-u}{\sigma})]^{-1/\xi}$.

Using $\lambda_u \equiv \Pr\{X > u\}$ one obtains the value x_m that is exceeded every m observation as solution of the following equation [11, S. 81]

$$\lambda_u \left[1 - \xi\Big(\frac{x_m - u}{\sigma}\Big)\right]^{-1/\xi} = \frac{1}{m}. \tag{5}$$

Direct solving yields $x_m = u + \frac{\sigma}{\xi}[(m\lambda_u)^\xi - 1]$. If $\xi = 0$ the solution reads $x_m = u + \sigma \ln(m\lambda_u)$ [11, S. 81]. Thus, a value as extreme as x_m will be exceeded every m observations. In applications it easier to interpret the return period in units of years. That is, which value will be exceeded every N years instead of every m observations. With n_y observations per year, $m = N \cdot n_y$ and the N-year return period reads $x_N = u + \frac{\sigma}{\xi}[(Nn_y\lambda_u)^\xi - 1]$ (or $x_N = u + \sigma \ln(Nn_y\lambda_u)$ if $\xi = 0$) [11, S. 82]. The original data can also be transformed to a return level plot by using the empirical distribution function (ECDF) $\hat{F}_i(x) = \frac{1}{i}\sum_l^i \mathbf{1}\{x_l < x\}$ with the indicator function $\mathbf{1}\{x\}$. The data pairs in a return level plot are then given by $((1-\hat{F}_i)^{-1}/n_y, x_i)$ and the regression reads $((1-\hat{F}_i)^{-1}/n_y, q + H^{-1}(1 - p_i/\tau, \hat{\xi}, \hat{\sigma}, 0))$ in which q is the τ-quantile of the data defining the threshold for 'extreme values' (we used $\tau = 0.9$ if not stated otherwise) and p_i denotes the probabilities of occurrence. Confidence bands were obtained via direct bootstrapping using a confidence level of $\alpha = 0.05$, that is the 'real' values should be contained in the confidence bands in 95% of the cases in which confidence bands are estimated [15].

3. Results

The present section contains results on the distribution of extreme wind speeds if wind power feed-in in different hours were uncorrelated 3.1, as opposed to the actually observed probability and return periods of long phases of low wind power feed-in presented in section 3.2. Similar results for phases of low residual load in Germany in 2006–2012 are presented in section 3.3. Finally, the representativeness of individual years concerning the distribution of phases of low wind power feed-in is given in section 3.4.

3.1. Distribution of wind speeds and wind power feed-in

Hourly wind speeds v and hourly wind power feed-in are approximately Weibull distributed $P(v) = \frac{\alpha}{v_0}\left(\frac{v}{v_0}\right)^{\alpha-1} \mathrm{e}^{-(v/v_0)^\alpha}$ with the cumulative distribution function (CDF) $F(v) = 1 - \exp[-(v/v_0)^\alpha]$. Here, v_0 denotes the scale and α the form parameter of the distribution. For the wind power feed-in in figure 2 the maximum likelihhod estimates for the parameters are given by $= v_0 = 0.193$ and $\alpha = 1.17$. If one neglects the correlation between wind speeds or power feed-in in subsequent hours, the probability of observing values below a threshold v over n hours was given by

$$W(n, 0 \leq V < v) = \left(1 - \mathrm{e}^{-(v/v_0)^\alpha}\right)^n \approx \mathrm{e}^{-\alpha n \ln(v/v_0)} \quad \text{for } v \ll v_0. \tag{6}$$

The probability for long wind phases above a threshold can similarly be calculated for uncorrelated Weibull distributed data: $W(n, v \leq V < \infty) = \mathrm{e}^{-(v/v_0)^{\alpha n}}$.

The probability of observing long phases of low wind speeds or wind power feed-in decreases exponentially with the duration for uncorrelated wind speeds and wind power feed-in. However, real wind and and wind power times series data are correlated. The effect of this correlation on the probability of long phases with low wind power feed-in is quite dramatic: The probability to remain for 24 hours in a phase of wind power feed-in below 8% of installed capacity would be 10^{-12} in stark contrast to the observed probabality of 1/4 (see figure 5 below). The highlights the importance of integrating correlation when analysing wind data.

3.2. Phases of low wind power feed-in

A growing share of wind power in the German energy system increases the importance of long phases of little wind power feed-in. As an example for such a phase, Figure 4 shows the normalised wind power feed-in in Germany for the first five weeks in January 2009. Phases of stronger and weak wind power feed-in are apparent. However, during the last week of January 2009 wind power feed-in was permanently below 16% of installed capacity and below eight percent for several days. Figure 4 shows possible thresholds for the definiton of 'low' wind power feed-in given by wind power feed-in below 2, 4, 8, 16, 32 or 64% of installed capacity. The latter two may not be considered lows (since they are above the mean wind power feed-in) but will serve as a reference below. These thresholds will be used for the analysis of low wind power feed-in phases further on.

The wind power feed-in data is browsed for phases below the mentioned threshold. The duration of these phases is collected and further analysed. Figure 5 shows the survivor function $S_u(t) = 1 - F_u(t)$ for the thresholds $u = 2, 4, 8, 16, 32, 64\%$ power feed-in of installed power p_0. Please note that figure 5 shows conditional probabilities since

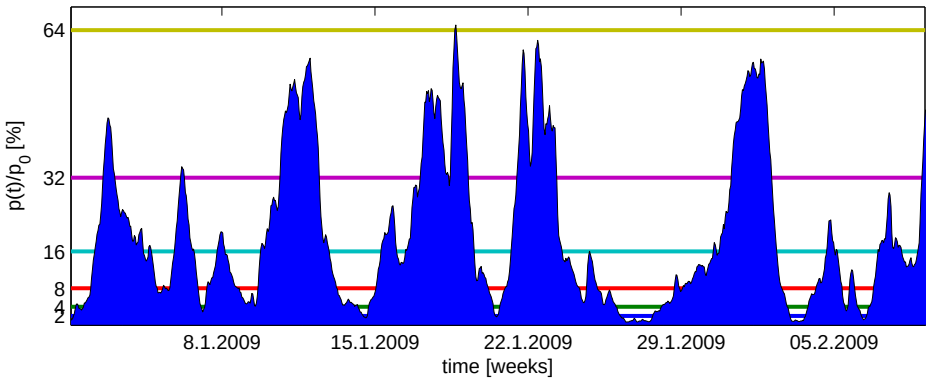

Figure 4: Normalised wind power feed-in in Germany in the first five eweeks of January 2009. A meterological inversion dominated German weather during the last week of January 2009 leading to very little (permanently below 16% (cyan line) and for several days below 8% (red line) of installed capacity) of total wind power feed-in in Germany.

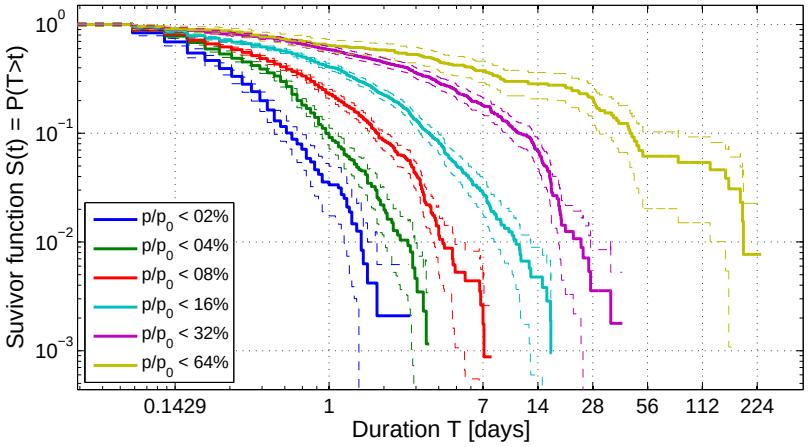

Figure 5: Survivor function fo long phases with little widn power feed-in (solid lines) with 95% confidence intervals.

$S_u(0) = 1 \forall u$ that is if the wind power feed-in is below the given threshold u, what is the probability to stay below the threshold for at least t days. The figure does not account for the fact that wind power feed-in below 32% of installed capacity occurs much more often than below 2%. Figure 5 has been chosen to make the different probability distributions comparable. As a comparison, the CDF in figure 2 (inset) shows that wind power feed-in below 1% p_0 is much less likely than below 32% p_0. The interpretation of figure 5 is as follows. Take as an example a phase of below 8% (of installed capacity of) wind power feed-in. Of all phases with below 8% about one out of 100 are at least four days long, that is the probability of observing a four day period of below 8% out of all below 8% periods is 10^{-2}. Figure 5 shows that long phases are more likely to observe if the threshold is raised. Furthermore the confidence band widths increase for longer

durations of low wind power feed-in phases since very long phases are more rare and the seven years of observation contain only a small number of these events.

More interesting is the extrapolation of extremely long phases of low wind power feed-in to even longer periods. We use extreme value theory to this end and performed a maximum likelihood fit of a generalised Pareto distribution to the longest ten percent of all periods of low wind power feed-in (i.e. of all durations longer than the 90% quantile of the durations). Figure 7 shows the return level plot for long phases of wind power feed-in below 8% threshold. The longest observed calm period in figure 7 was seven days

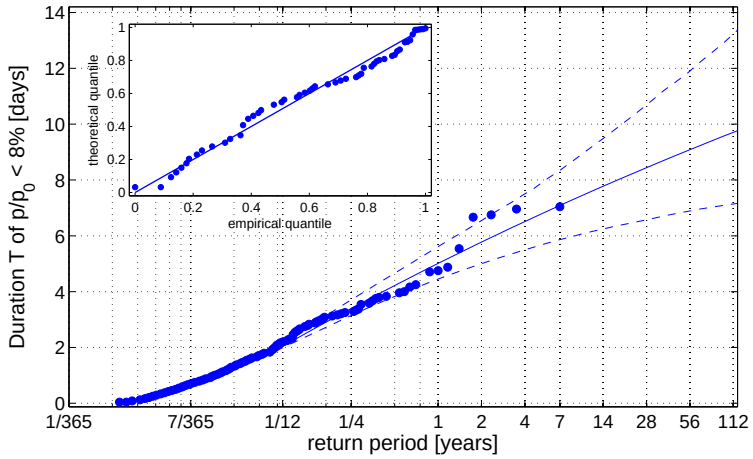

Figure 6: Return period plot for long periods of below 8% wind power feed-in (circles) and regression of extreme values based on generalised Pareto distribution (solid blue line) including a 95% confidence band (dashed lines). The threshold for an extreme period is 1.4 days of length and 166 extreme periods have been observed. *Inset*: Quantile plot for the extreme value regression (cp. figure 6) of long periods with wind power feed-in below 8 % installed capacity (circles).

long and has a numerical return period of seven years since it occurred only once during the seven years of data 2006–2012. Furthermore, longer calms of wind power feed-in of more than one week duration occur quite frequently. The GPD fit shows that periods of more than ten days every 25 years are consistent with the data (i.e. within the 95% confidence band). Furthermore, a one-hundred-year calm in wind power feed-in could last for almost two weeks. The inset of figure 7 shows acceptable agreement between the empirical and theoretical quantiles of the long periods (above the 90% quantile) of phases with low wind power feed-in and the fitted GPD.

Similar return level plots including GPD estimates for larger magnitude calms in wind power feed-in have been performed for other thresholds 2, 4, 8, 16, and 32% of installed capacity (horizontal lines in figure 4) and are shown in figure 7. The title of each plot contains the threshold value as duration measured in days using the 90% quantile threshold and are given by 0.6, 0.9, 1.8, 3.5, and 11.1 days for the 2, 4, 8, 16, and 32% thresholds together with the sample size for the GPD fit ($n = 48$, 86, 113, 105, and 56 phases). The 64% threshold has been omitted since the number of data points was not sufficient for reliable GPD parameter estimates.

Figure 7 demonstrates that a phase of wind power feed-in below 2% of installed capacity can easily take a duration of two days. A hundred-year calm below 2% of 2–4

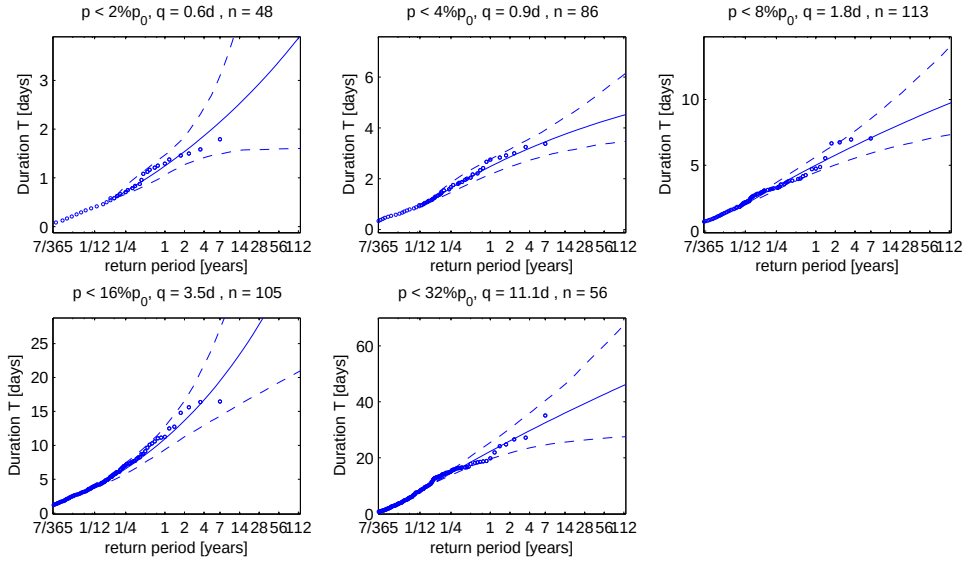

Figure 7: Return period plot for long periods of below 2% (top left), 4% (top centre), 8% (top right), 16% (bootom left) and 32% (bottom centre panel) of wind power feed-in (circles) and regression of extreme values based on generalised Pareto distribution (solid blue line) including a 95% confidence band (dashed lines). The threshold for an extreme period is 1.4 days of length and 166 extreme periods have been observed.

days is consistent with the data. Similarly, a wind power feed-in below 4% of installed wind capacity is quite frequently longer than two days. The observed and possible durations of low wind power feed-in grow longer as the threshold level for 'low' is raised. Several phases of more than two weeks with below 16% wind power feed-in have been observed several times in Germany 2006–2012 (note that this is still below the average wind power feed-in of 18.1%). An extremely long yet possible within 50 years low wind power feed-in phase could extend over more than a month.

Our results show that phases of low wind power feed-in can easily extend over many hours or several days depending on the definition of 'low' i.e. the threshold applied. A more systematic analysis of typical durations of low wind power phases in shown in figure 8. The figure contains the median duration of all observed phases of below a threshold as a function of the threshold in percent of installed capacity. Also shown in figure 8 are the 25%- and 75%-quantile of the distribution of low wind power phase durations. All quantiles grow approximately linearly with the threshold. Furthermore, the inter-quartile range (the distance between the 25%- and 75%-quantiles) grows as well, indicating that the distributions are more right skewed the higher the threshold. The linear dependence of the median duration $\bar{T}_m$ of a phase on the threshold is approximately given by $\bar{T}_m = 1.0 \cdot p_\tau + 2.0$ in which p_τ is the threshold in percent of installed capacity. We thus find the median duration of low wind power feed-in phases to grow linearly with the threshold: Phases with a wind power feed-in of less than two percent of installed power are typically four hours long and phases with less than five percent feed-in are on average seven hours long.

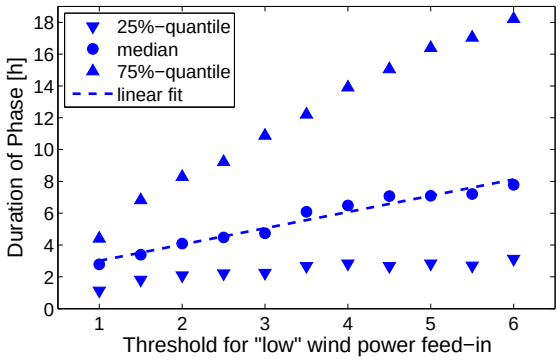

Figure 8: Duration of phases of low wind power feed-in in Germany 2006–2012 as a function of threshold power (in percent of installed capacity) for the defintion of "low" wind power feed-in. Lower quartile ($\triangledown$), median values ($\circ$) and upper quartiles ($\triangle$) are shown together with a linear regression of the median value (dashed line).

3.3. Phases of Low Residual Load

We now turn to long phases of low residual power. We analysed residual load data for the same time period 2006–2012 in Germany. During that period the PV and wind power capacity increased and the individual years are not directly comparable with the respect to the residual load. Yet in a future energy system residual load will spread even more and it is interesting to understand the present day situation before analysing a future energy system.

The seven years of residual load data 2006–2012 in Germany have been searched numerically for phases with residual load below certain threshold. We use $u = 35$, 40, 49, and 60 GW as threshold values roughly corresponding to the 3, 8, 32, and 64%-qunatiles. The duration of the phases have been recorded and analysed. Figure 5 shows the survivor functions for phases of low residual load. Note that these have been normalised to $S_u(0) = 1\,\forall u$, that is they show what fraction of all phases below a threshold lasts at least t hours. We observe again that the likelihood of long phases of low residual load increases with the threshold value for 'low'. For example, a phase of two days duration happens only in every 200th phase with below 40 GW residual load ($S(1d) \approx 5 \cdot 10^{-3}$), in every 50th phase with residual load below 49 GW ($S(1d) \approx 0.02$) and in every tenth phase of residual load below 60 GW ($S(1d) \approx 0.1$). Furthermore, the width of the confidence bands increases for longer durations as the numbe rof observations with such long duration decreases. In particular, the data does not suffice to estimate reliable differences between the 35 GW and 40 GW survivor functions at about one day length.

We also used maximum likelihood estimators to analyse the probability of extremely long phases of low residual load. Figure 10 shows the return level plot for phases of below 35 GW (left panel) and 49 GW (right panel) residual load. We used the 90%-quantile as threshold for 35 GW phases and, since more data was available, the 97%-quantile as threshold for the 49 GW phases. The quantile plot shows acceptable agreement but the number of observations is limited in the case of below 38 GW residual loads as the wide confidence bands indicate. The situation is slightly better for the below 49 GW residual load data. The return level plot demonstrates that during the seven years of observation

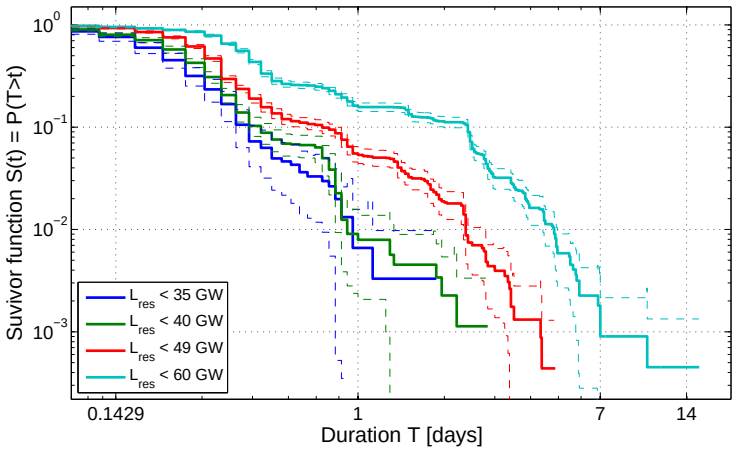

Figure 9: Survivor function of long phases with low risdual load (solid lines) with 95% confidence intervals (dashed lines) for 'low' with the thresholds $u = 35$ (blue), 40 (green), 49 (red) and 60 GW (cyan).

the longest phase with residual load smaller than 35 GW was about a whole day long and that up to three days were consistent with the data if the energy system did not alter. For a threshold of 49 GW several days with residual load below that threshold have been observed. (Note that 49 GW corresponds to the 32%-quantile and is still clearly below the average residual load of 55 GW during the observation period.) The extrapolation of the past residual load is of course not reliable considering the future increase of renewable energy generation. However, the noteworthy duration of phases below fixed thresholds even in present day residual loads demonstrates the effect of renewable generation on residual load even today.

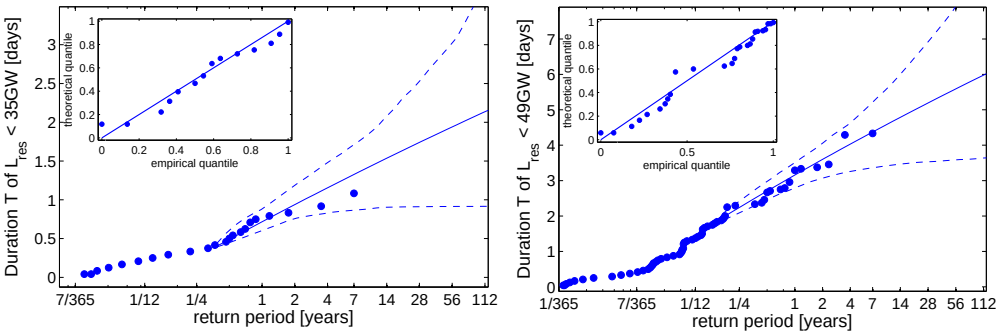

Figure 10: Return level plot for long periods of below 35 GW (left panel) and below 49 GW (right panel) phases of residual load. The orginal data (circles) and a GPD fit (solid line) including a 95% confidence band (dashed lines) are shown. *Insets*: Quantile plot for the extreme value regressions.

3.4. Representativeness of individual years

Energy system analysis uses historical weather or renewable generation time series to analyse possible future energy systems. In many cases, historical data from a fixed year

is rescaled to future renewable generation or renewable capacity. However, the sensitivity of the results on the weather (or generation) time series data is not analysed. For the case of long periods with low wind power generation (normalised to installed capacity), this raises the question of representativeness of individual years and will be discussed in the present section.

We analysed the seven years of observation individually for phases of low wind power feed-in and compared them to the seven-year average. We measure the similarity of an individual year to the complete data set 2006–2012 by a χ^2 measure and compare the mean duration of phases with wind power feed-in below a bound to the long time average of that duration. We thus analyse the representativeness with respect to phase duration not with resepect to the number of phases. The similarity measure is defined as $\chi^2 = \sum_i (o_i - e_i)^2/e_i$ in which $e_i = \frac{1}{N}\sum_l^N \ln(t_{li})$ is the long time average of the (logarithm of) individual durations t_{li} below the ith threshold of all years, $o_i = \frac{1}{n}\sum_l^n \ln(t_{li})$ the observed value of averages in that particular year and i enumerates the thresholds. We used the logarithm of the durations to acknolwedge for the right-skewedness of the distribution of durations (as indicated by figure 5). Years with durations very similar to the long time average will have a low χ^2 value, years with non-typical durations a larger value. We used thresholds $\tau_i = 1, 1.5, \ldots, 6.0\%$ of installed capacity for wind power feed-in. The maximal value 6% wind power feed-in of installed capacity corresponds to the 25%-quantile of the observed wind power feed-in and guarantees that we are analysing clearly low wind power feed-in. The steps of 0.5% ensure a resolution high enough to analyse different phases but a large enough number of phases within the different thresholds.

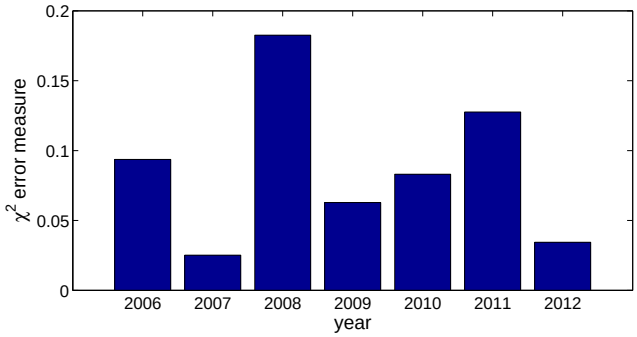

Figure 11: Similarity of individual years with all years in terms of distribution of phases of little wind power feed-in Germany.

Figure 11 shows that the years 2007 and 2012 show the highest similarity to the long year behaviour for the duration of phases with low wind power feed-in. The lowest similarity exhibit the years 2008 and 2011. However, the the χ^2 measure in figure 11 takes into account only the duration of low wind power phases. Further research should compare these results to number of such phases and the average wind power in these years to find which years show the highest similarity to several aspects of relevance for energy economics.

4. Summary and Discussion

We analysed phases of low wind power feed-in and low residual load in Germany 2006–2012. Our results show that a period of wind power feed-in below eight percent of installed power that lasts one week occurs every two years and a period of more than ten days occurs every ten years. Furthermore, we find the average duration of low wind power feed-in phase to grow linearly with the threshold: phases with a wind power feed-in of less than two percent of installed power are typically four hours long and phases with less than five percent feed-in are on average seven hours long. We did not study solar power individually which could compensate low wind power (the residual load of course contains the effect of solar power to some extend). In addition, please note that we analysed historical residual load data. In this period, the spread between minimal and maximal residual load was limited. In a future energy system, periods of negative residual load and a growing spread in residual load can be expected. This is not present in the historical data.

The effects on energy system analysis are complex. Energy system models optimise the whole system (under given constraints) without detailed analysis of intermediate steps. For future energy systems, the duration and frequency of phases with low wind power feed-in and thus low residual load are a major factor determining the economics of energy storages but the detailed steps are difficult to analyse. In this context, our results show that long phases of low wind power are quite normal and that individual years differ in the duration of wind power feed-in phases.

References

[1] Sensfuß, F., Ragwitz, M., Genoese, M., and Möst, D. (2007). "Agent-based simulation of electricity markets: a literature review". Working paper sustainability and innovation No. S5/2007, Karlsruhe, Fraunhofer ISI

[2] Jebaraj, S., and Iniyan, S. (2006). "A review of energy models." Renewable and Sustainable Energy Reviews 10(4) 281-311.

[3] Cook, N. J. "Towards better estimation of extreme winds." Journal of Wind Engineering and Industrial Aerodynamics 9(3), 295-323.

[4] Palutikof, J. P., et al. "A review of methods to calculate extreme wind speeds." Meteorological applications 6 (2), 119-132.

[5] Simiu, E., and Heckert, N. A. (1996). "Extreme wind distribution tails: a 'peaks over threshold' approach." Journal of Structural Engineering 122.5: 539-547.

[6] Conradsen, K., Nielsen, L. B., and Prahm, L. P. (1984). "Review of Weibull statistics for estimation of wind speed distributions." Journal of Climate and Applied Meteorology, 23(8), 1173-1183.

[7] Nolan, P., Lynch, P., McGrath, R., Semmler, T. and Wang, S. (2012). "Simulating climate change and its effects on the wind energy resource of Ireland." Wind Energy 15(4), 593-608.

[8] `http://www.offshore-windenergie.net/windparks`, last retrieved: 1/4/2014.

[9] `http://www.netztransparenz.de/de/Windenergie_Hochrechnung.htm`, formally `www.eeg-kwk.net`, last retrieved: 1/4/2014.

[10] `https://www.entsoe.eu/data/data-portal/consumption/`, last retrieved: 1/4/2014.

[11] S. Coles. *An introduction to statistical modeling of extreme values*. Springer, 2001.

[12] Perrin, O., Rootzn, H., and Taesler, R. (2006). "A discussion of statistical methods used to estimate extreme wind speeds." Theoretical and applied climatology 85(3-4), 203-215.

[13] `http://www.wind-energie.de/infocenter/statistiken/deutschland/installierte-windenergieleistung-deutschland` last retrieved: 1/4/2014.

[14] Bundesverband der Energie- und Wasserwirtschaft e. V. "Net electricity consumption in Germany 1999–2012". `http://www.bdew.de/internet.nsf/id/de_energiedaten`, last retrieved: 1/4/2014.

[15] L. Fahrmeir (2009). *Statistik*. Springer, Berlin.

[16] J.F. Lawless (2004). *Statistical Models and Methods for Lifetime Data*, Wiley, New York.